



HAL
open science

Review on the research of hydrogen storage system fast refueling in fuel cell vehicle

Mengxiao Li, Yunfeng Bai, Caizhi Zhang, Yuxi Song, Shangfeng Jiang, Didier Grouset, Mingjun Zhang

► To cite this version:

Mengxiao Li, Yunfeng Bai, Caizhi Zhang, Yuxi Song, Shangfeng Jiang, et al.. Review on the research of hydrogen storage system fast refueling in fuel cell vehicle: Review. *International Journal of Hydrogen Energy*, 2019, 44 (21), pp.10677-10693. 10.1016/j.ijhydene.2019.02.208 . hal-02081359

HAL Id: hal-02081359

<https://imt-mines-albi.hal.science/hal-02081359>

Submitted on 1 Apr 2019

HAL is a multi-disciplinary open access archive for the deposit and dissemination of scientific research documents, whether they are published or not. The documents may come from teaching and research institutions in France or abroad, or from public or private research centers.

L'archive ouverte pluridisciplinaire **HAL**, est destinée au dépôt et à la diffusion de documents scientifiques de niveau recherche, publiés ou non, émanant des établissements d'enseignement et de recherche français ou étrangers, des laboratoires publics ou privés.

Review on the research of hydrogen storage system fast refueling in fuel cell vehicle

Mengxiao Li ^{a,1}, Yunfeng Bai ^{a,1}, Caizhi Zhang ^{a,*}, Yuxi Song ^a,
Shangfeng Jiang ^b, Didier Grouset ^{c,**}, Mingjun Zhang ^d

^a School of Automotive Engineering, The State Key Laboratory of Mechanical Transmissions, Chongqing Automotive Collaborative Innovation Centre, Chongqing University, Chongqing, 400044, China

^b Zhengzhou Yutong Bus Co. Ltd., Yutong Industrial Park, Yutong Road, Zhengzhou, Henan Province, 450061, China

^c RAPSODEE, UMR CNRS 5302, IMT Mines-Albi, Campus Jarlard, 81013 Albi, CT Cedex 09, France

^d Beijing PERIC Hydrogen Technologies Co. Ltd, Qingnian Road, Damei Center, Chaoyang District, Beijing, 100123, China

ABSTRACT

A comprehensive review of the hydrogen storage systems and investigations performed in search for development of fast refueling technology for fuel cell vehicles are presented. Nowadays, hydrogen is considered as a good and promising energy carrier and can be stored in gaseous, liquid or solid state. Among the three ways, high pressure (such as 35 MPa or 70 MPa) appears to be the most suitable method for transportation due to its technical simplicity, high reliability, high energy efficiency and affordability. However, the refueling of high pressure hydrogen can cause a rapid increase of inner temperature of the storage cylinder, which may result not only in a decrease of the state of charge (SOC) but also in damages to the tank walls and finally to safety problems. In this paper, the theoretical analysis, experiments and simulations on the factors related to the fast refueling, such as initial pressure, initial temperature, filling rate and ambient temperature, are reviewed and analyzed. Understanding the potential relationships between these parameters and the temperature rise may shed a light in developing novel controlling strategies and innovative routes for hydrogen tank fast filling.

Keywords:

Hydrogen storage

Fast filling

Temperature rise

CFD

Strategy

Contents

Introduction	00
Hydrogen storage systems	00
Comparison of hydrogen storage ways	00
Comparison of hydrogen storage vessel	00
Effects of thermo-mechanical effects on hydrogen storage tanks	00
Theoretical analysis	00

* Corresponding author.

** Corresponding author.

E-mail addresses: czzhang@cqu.edu.cn (C. Zhang), grouset@mines-albi.fr (D. Grouset).

The effects of parameters on temperature rise during refueling	00
Effect of initial pressure	00
Effect of filling rate	00
Effect of inlet temperature (or feeding temperature)	00
Effect of cylinder dimension or cylinder type	00
Effect of initial and ambient temperature	00
CFD simulations	00
Geometry grid	00
Turbulence models	00
Real gas model	00
Definite conditions	00
The safety and fast filling strategies	00
Filling rate control strategy	00
Refueling with multi-stage initial pressures	00
Determining pre-cooling temperature from refueling parameters	00
Conclusion	00
Acknowledgments	00
References	00

Introduction

The proton exchange membrane (PEM) fuel cells enjoy the merits of low operating temperature, low noise, quick startup and high efficiency [1,2]. PEMFCs can generate powers from a few Watt to hundreds of kilo-Watt and are already in the commercialization stage in three areas: transportation, stationary power system and portable market [3,4]. The most in sight and promising application field of PEM fuel cells is in the transportation [5], including automobiles, buses, scooters, boats and unmanned aerial vehicles (UAV) [6]. During the recent years, almost all major car manufacturers have declared intending or being manufacturing FC vehicles. Hydrogen energy is a high promising candidate as an energy carrier for fuel cell vehicle since it can be produced locally from a variety of renewable sources with nontoxic, noncorrosive, environment friendly, high efficiency processes [7]. Nevertheless, there is no easy or immediate solution for on-board hydrogen storage currently. Hydrogen storage is an important issue that restricts the widely application of fuel cell vehicles.

At present, the possible storage methods of hydrogen are compressed gas, cryogenic liquid and metal hydride [8]. In transportation field, the compressed gas storage method is more common than other methods due to its technical simplicity, high reliability, acceptable efficiency and affordability [7,9,10]. Nevertheless, considering the process of fast refueling, the temperature rise is a significant issue which is caused by three main thermodynamic phenomena [11]. Firstly, the kinetic energy of the fast-flowing hydrogen converted into the internal energy gas generates lots of heat in the process of filling. Secondly, the hydrogen expanding through a throttling valve results in an increase of temperature, called as Joule-Thomson effect. Thirdly, the compression of hydrogen in the tank during its filling causes a temperature rise, too. Moreover, the temperature rise not only reduce the SOC of the hydrogen tank but could also bring safety hazards. Thus,

hydrogen fast charging is a serious process that needs to be considered with care to reduce risks.

In practice, several parameters (e.g. the initial pressure, initial temperature of hydrogen, the filling rate and so on) have various influences on the final temperature. To investigate the relationships between the temperature and the parameters, several experiments and simulations investigated the temperature rise within a compressed cylinder. In order to study the thermal behavior during hydrogen fast filling process, Johnson et al. [10] developed one-dimensional and 3D models and conducted experiments for comparing. The mass flow rate has a more significant effect than other parameters. However, drivers do not expected to spend a longer time for refueling the hydrogen vehicles compared to the conventional liquid fuel powered vehicles [12]. Nevertheless, the temperature rise during the fast filling process is a serious issue and it is significant to develop an effective strategy to achieve the safe and fast refueling. In view of the influence of initial gas temperature on temperature rise, precooling measures are adopted to improve the fast filling of hydrogen and have been validated to be the most effective way to reduce the final temperature. In addition, the process of multi-stage filling is adopted to decrease the energy consumption and Guo et al. [13] designed a dynamic simulation module to optimize the gas cycling test system in a view of energy consumption reduction.

The construction and operation of refueling stations hydrogen refueling stations requires high capital investment [14–16]. Adopting appropriate operational strategies could reduce capital investment while improving equipment utilization. Hence, the research of fast filling strategies is necessary. At present, the process of multi-stage filling combined with the measure of precooling have been widely applied in most filling stations. The precooling of hydrogen could decrease the temperature rise effectively and the process of multi-stage filling could reduce the energy consumption. The configurations of off-site hydrogen generation filling station

are shown as Fig. 1 [8]. The hydrogen source is the high-pressure tube-trailers. The tube trailers can be used to supply hydrogen to the buffer storage vessels through the compressor. The high-pressure tubes (25 MPa or higher) on the tube trailer can also be used to initially charge the vehicle's tank before the pressure drops. Then the suitable control strategy is adopted to refuel the vehicle tank successively from the multi-stage hydrogen storage system. The pre-cooling system can be determined whether to enable or not according to the ambient temperature.

In this paper, the current methods on controlling the temperature rise during refueling, such as changing the gas initial temperature, initial pressure, ambient temperature and pre-cooling process are reviewed. The organization of this paper is as follows. Section [Hydrogen storage systems](#) presents hydrogen storage systems, such as compressed hydrogen storage, liquid hydrogen storage and metal hydride hydrogen storage. Based on compressed hydrogen storage, four different types of tanks are compared. The thermodynamic mechanism and theoretical analysis of temperature rise are reviewed in Section [Theoretical analysis](#). Section [The effects of parameters on temperature rise during refueling](#) summarizes the current experiments and simulations on fast and safe hydrogen refueling technology. Section [CFD simulations](#) summarizes a series of CFD models on the flow field and temperature field during the process of hydrogen charging. Section [The safety and fast filling strategies](#) studies the safety and fast filling strategies. Finally, conclusion is given in Section [Conclusion](#).

Hydrogen storage systems

Comparison of hydrogen storage ways

In the development of hydrogen energy, storage is considered as a key issue for the widespread use in transportation, stationary power system and portable market [17,18]. At present, the most common ways to store hydrogen are compressed

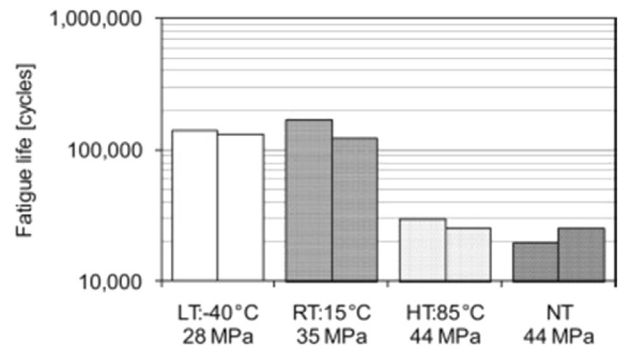


Fig. 2 – Fatigue life under each condition [50].

hydrogen storage, cryogenic liquid and metal hydride [19,20]. Recently, Abdalla et al. [21] summarized the storage methods of hydrogen in one of their studies, covering compressed hydrogen, liquefied hydrogen, metal hydride, carbon nanotubes, liquid organic hydrogen carrier and metal-organic framework. There is amount of ways for storing hydrogen fuel in different forms as show in Table 1 [22–26]. Compared with the above several methods, compressed gas storage is more popular due to its technical simplicity, high reliability, acceptable efficiency and affordability [27].

Comparison of hydrogen storage vessel

The key technology for the widespread use of compressed hydrogen is the storage vessel. The requirements of the material used in the hydrogen storage vessel are: safe, reliable, cost effective and any strong interaction with hydrogen or any reaction. As early as 1880, pressure vessel use has been reported: hydrogen was stored in wrought iron vessel at 12 MPa for military application [19]. Currently, hydrogen vessels are mainly divided into 4 different types (Type I to Type IV) as shown in Table 2 [21,28–30]. It is the most mature and commonly adopted solution of hydrogen storage in vehicles [7,31]. Usually hydrogen cylinders can be pressurized up to

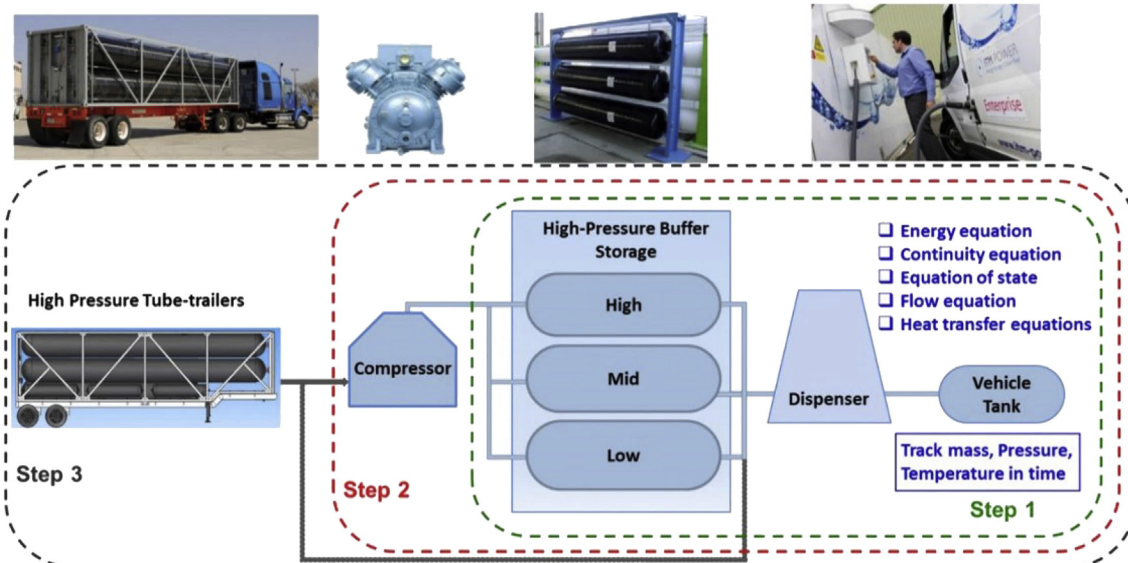


Fig. 1 – Schematic representation of the refueling station components [8].

Table 1 – Hydrogen storage types and comparisons.

Category	Type	Advantages	Issues
Gas storage	Compressed hydrogen	High efficiency, convenient, mature technology.	Expensive cylinder and the immature technology of fast filling.
Liquid storage	Liquid hydrogen	High liquid density and storage efficiency.	Large consume of energy and time, low temperature.
Carbon nanotubes	Gaseous hydrogen	Highly porous structure and particular interaction between carbon atoms and gas molecules.	Immature technology and hydrogen capacity depends on many factors.
Chemical storage (metal hydride)	MgH ₂ CaH ₂ NaH	High safety, high purity of hydrogen, good reversible cycle performance, large volume of hydrogen density.	Absorbing impurities, reducing the hydrogen capacity and the lifetime of tank.
Physical storage (metal organic framework)	Porous coordination network	Highly porous, high uptake of H ₂ and specific surface areas.	Hydrogen storage temperature is far below operating temperature.

25 MPa, 35 MPa or 70 MPa. Considering the driving range and limited space in vehicle, 70 MPa is to be the most economic pressure for onboard storage [28,32].

Comparing the above four types, it is found that Type I and Type II cannot be used in vehicles due to low hydrogen storage density and serious hydrogen embrittlement problems. In the industry of fuel cell vehicles (FCVs), Type III and Type IV are widely used for weight minimization [7,31,33]. However, Type III and IV have different behavior with respect to temperature rise due to the material differences. Some characteristic property data of Type III and IV are shown in Table 3, according to Ref. [29].

In China, the technology development of Type III is relatively mature. Among them, the 35 MPa vessel has been widely used in fuel cell vehicles in recent years and the 70 MPa vessel is near the market. However, the shortage of carbon fiber and resin, and the performance of these materials block the development of hydrogen vessel. The Type IV vessel have only recently been developed [28].

At present, most of the developed fuel cell vehicles use high-pressure cylinders to store hydrogen on board. Table 4 documents the key parameters of several fuel cell vehicles. The Honda FCX is equipped with two 35 MPa tank that can achieve a 156.6 L hydrogen capacity [34]. Toyota FCHV-adv used four type IV 70 MPa tanks to supply hydrogen for its fuel cell stack, the total volume of the four tanks is 156 L, which could achieve a driving range in practical driving conditions of at least 500 km with a roughly 10 min fueling time [35,36]. In order to reduce the weight, size and cost of the high-pressure hydrogen storage system, Toyota “Mirai” employs two new larger diameter tanks (60 L and 62.4 L). They can store nearly 5 kg hydrogen in 3 min and provide a driving range of approximately 500 km [36]. Recently, Hyundai released a new fuel cell SUV, NEXO, which features three same fuel tanks with a total capacity of 156 L and 6.3 kg and with a fueling time of 5 min. It is said that the newly fuel cell vehicle can achieve a driving range of up to 800 km under current NEDC testing cycle.

Effects of thermo-mechanical effects on hydrogen storage tanks

In the application process, compressed-hydrogen tanks for vehicles are fatigued by cycles of filling and consumption

[46,47]. Pressure vessels are directly subjected to the cyclic loading of both high pressure and extreme temperature. The temperature in the tank increases significantly during the fast filling process but declines in the process of gas usage routine. The violent changes of temperature can lead to severe thermal stress due to the mismatch in the coefficient of thermal expansion of adjacent plies with different fiber orientations, which accompanied by internal pressure during numerous charge-discharge processes. The superposition of thermal stress and internal pressure will cause obvious lamination damage in the form of micro-cracks in the resin, and then lead to the failure of the composite material. Furthermore, the temperature changes will seriously affect mechanical properties of the epoxy resin and carbon fibers. The fracture toughness of the epoxy resin matrix will decrease seriously at low temperatures, while the inter laminar shear strength of the composites will dramatically decrease at high temperature. Thus, the strength and fatigue life of the composite vessel are seriously affected [48].

Indeed, risks of an early failure appear when the type III vessels are subjected to cyclic pressures and permeation problems happen for the type IV [49]. Tomioka et al. investigate the influence of the environmental temperature on the fatigue strength of compressed-hydrogen tanks (Type III and Type IV). The fatigue strength of the Type III tank decreases in a low temperature environment and increases in a high-temperature environment. However, the fatigue strength of type IV decreased in a high-temperature environment [50]. The temperature rise result in stratification between the plastic liner and the composite wrapping materials of type IV tank [28]. Some experimental researches on the fatigue of composite hydrogen storage vessels are shown in Table 5.

Theoretical analysis

Temperature of the cylinder could maintain within the specified threshold after refueling is expected. Therefore, investigating the mechanism of temperature rise during the fast filling process becomes the focus of research. There is a rapid increase in hydrogen temperature due to three main thermodynamic phenomena during hydrogen filling process [51]. Firstly, the kinetic energy of the fast-flowing hydrogen

Table 2 – Different types of hydrogen compressed tank.

Cylinder types	Materials	Features	Applications	Hydrogen storage pressure and mass percent (WT%)
Type I	All metal	Heavy, internal corrosion	For industrial, not suited for vehicular use	17.5–20 MPa 1 WT% [21]
Type II	Metal liner with hoop wrapping	Heavy, short life due to internal corrosion	Not suited for vehicular use	26.3–30 MPa
Type III	Metal liner with full composite wrapping	Lightness, high burst pressure, no permeation, galvanic corrosion between liner and fiber	Suited for vehicular use. 25–75% mass gain over I and II	35 MPa: 3.9 WT% –70 MPa: 5 WT%
Type IV	Plastic liner with full composite wrapping	Lightness, lower burst pressure. Permeation through liner, high durability against repeated charging Simple manufacturability	Longer life than Type III (no creep fatigue).	70 MPa: more than 5 WT%,

converted into the internal energy gas generates lots of heat in the process of filling. Secondly, the compression of hydrogen in the tank during its filling causes a temperature rise, which is the most important among all factors leading to temperature rise. Thirdly, the hydrogen expanding through a throttling valve results in an increase of temperature, called as Joule-Thomson effect. Other than general gases, the Joule-Thompson negative effect appears during hydrogen expand through a throttling valve due to its unique nature. In the meantime, a good news is that part of the heat in the cylinder may transfer to the ambient due to the difference in temperature. Nevertheless, most part of the heat is stored in the wall of the cylinder, which lead to the temperature rise of the cylinder. Taking into account the simplicity of the model, the hydrogen filling process could be simplified as Fig. 3.

The theoretical analysis is mainly based on the simplified thermodynamic model. The energy and mass conservation equations combined with the real gas equation of state to obtain the relationship of the temperature and pressure in initial state and final state respectively. In the theoretical model of Liu et al. [51] as shown in Table 6. The internal energy and kinetic energy of hydrogen were considered. Considering that refueling time is short and assuming it an adiabatic process, the heat transferring to ambient is ignored. Another assumption is that initial temperature within the cylinder equals to hydrogen temperature before filling. The result shows the final hydrogen temperature in the cylinder could be calculated accurately with the relative parameters in the simplified process. In another work accomplished by M. Hosseini et al. [52], additional work have been done is that the exergy of the hydrogen in the cylinder is also investigated, which could illustrate the thermodynamic mechanism more comprehensively. Yang et al. [53] carried out

the model analysis with the gaseous hydrogen treated as an ideal or a non-ideal gas and the refueling process analyzed based on adiabatic, isothermal, or diathermal condition of the cylinder. A constant feed-rate is assumed in the analysis. The consequence shows that the adiabatic and isothermal conditions were the lower and upper bounds of the filling time for a given final target pressure. Assuming that the specific heat is constant ($C_v = 5.178$ kJ/kg K), Wang et al. [54] developed the thermodynamical model based on the conservation equation of energy. The mass and temperature after filling could be obtained.

The theoretical analysis shows the change of temperature clearly with mathematical formula. As we can see, the temperature rise of hydrogen is mainly determined by filling parameters. In addition, some other parameters such as the geometrical parameters of the cylinder may also affect the state of cylinder after filling. Hence, further research of the effects of these parameters is required.

The effects of parameters on temperature rise during refueling

The gas temperature may rise significantly during the high-pressure hydrogen cylinder refueling and lead to a failure of the hydrogen storage tank [29]. Furthermore, the high temperature also reduces the hydrogen density in the tank, resulting in a reduction of the final mass delivery and in turn, decreasing the driving range of the hydrogen vehicles. Hence, the study of temperature rise during refueling is a significant concern regarding hydrogen safety [55]. Syrian et al. [29] and Zheng et al. [7] carried out experimental studies and CFD simulations on type III vessels. Kim et al. [28], Galassi et al. [17] and Melideo et al. [56] worked on type IV vessels. Heitsch et al. [57] and Melideo et al. [12] compared the influence of the type (III or IV) on temperature rise in cylinders during fast refueling. For safety concern, the GTR-HFCV [58], the SAE-J2579 [59] and the ISO-15869 [60] have restricted the maximum wall temperature inside the hydrogen vessel below 358 K and the maximum fueling pressure has to limited below 125% of the designed pressure. Therefore, the temperature rise in the hydrogen vessel during the fueling process has to be controlled within these allowed limitations. Investigating the

Table 3 – The property of type III and type IV tank.

Cylinder types	Thermal conductivity (W/mK)	Density (Kg/m ³)	Specific heat capacity (J/kg K)
Type III: Metal liner	167	2730	900
Type III: Laminate	1	1494	938
Type IV: Plastic liner	0.3	947	1880
Type IV: Laminate	1.5	1600	1400

Table 4 – Specifications of several fuel cell vehicles [14,37–45].

Vehicle name	Year	Max. output (bhp/kw)	Total volume of tanks (L) and tank' type	Driving range (km)
Honda FCX 2nd Generation	2004	/	156.6	430
Honda FCX Clarity	2008	134/100	171	386
Toyota FCV-adv	2008	121/90	156 (type 4)	483
Toyota Mirai	2014	153/144	122.4 (type 4)	502
Hyundai ix35	2014	136/100	5.63 kg under 70 MPa	594
Hyundai NEXO	2018	161/95	156	595.5

fueling parameters, such as the initial pressure, initial gas temperature, ambient temperature, filling rate and even the cylinder dimensions, is very significant to control the final tank gas and wall temperature below 85 °C effectively.

Effect of initial pressure

During the fast filling process, the initial pressure in the cylinder has a significant effect to the final temperature. Higher initial pressure means more hydrogen initially stored in the tank and a lower pressure ratio between final and initial pressure ration, which both can mitigate the temperature rise during refueling [61]. In order to estimate the influence of the different initial pressures on the final temperature, several experiments and simulations completed by researchers are shown in Table 7.

In order to study the relationship between the initial pressure and the final temperature during the refueling process, various experiments with different facilities and conditions have been conducted. The negative influence of the initial pressure on the final temperature can be seen. An

experimental system built by Zheng et al. [7] was equipped with sixteen thermocouples and a pre-cooling system. Their results indicated the final temperature of the gas decreases about 4.5 K when the initial pressure increases 5 MPa. In the meanwhile, other experiments developed by Kim et al. [28] and Liu et al. [51] also validates the maximum temperature decreases almost linearly as the initial gas pressure increases. Grouset et al. [64], using a 0D model for the gas and a 1D model for the tank wall, also reports a linear variation with a sensitivity coefficient of 1.06 °C/MPa at 70 MPa and -1.64 °C/MPa at 70 MPa. Therefore, the initial pressure has an important effect on the temperature rise. In order to limit the filling temperature under the threshold, the optimal filling initial pressure must be considered combined with other parameters.

Effect of filling rate

With the wide application of hydrogen energy in automobiles [5], the length of the fill time becomes the focus of people's attention. However, increasing the filling rate to minimize the fill time may result in a final temperature exceeding the

Table 5 – Experimental researches on the fatigue of hydrogen storage vessels.

Author	Experiment	Parameter	Frequency	Results analysis
Chuan-xiang ZHENG [48]	70-MPa Fatigue test system using hydrogen as medium	The highest testing pressure of the system: 70 MPa. The greatest hydrogen mass flow rate: 3.24 kg/min.	10 min/cycle After 500 times fatigue test, the bursting characteristics was checked Another sample vessel was tested in this system until failure.	The experimental results show that hydrogen environment fatigue affects the ultimate strength of the composite vessels: nearly 15% drop off compared with design pressure. The fatigue life of another test sample is 5122 times which is much shorter than that under hydraulic fatigue test (about 12,000 times).
Tomioka [50]	Hydraulic pressure-cycle tests to investigate the fatigue life of Type III tanks when environmental temperature and filling pressure are changed.	Low temperatures (-40 °C, 28 MPa) Room temperature (15 °C, 35 MPa) High temperatures (85 °C, 44 MPa) Normal temperature (15 °C–35 °C, (with no temperature control), 44 MPa)	1 min/cycle 10,000 cycles	The fatigue life at high temperatures (85 °C, 44 MPa) was shorter than that under other conditions. As shown in Fig. 2.
Tomioka [46]	Hydraulic pressure-cycle tests with varying environmental temperatures were conducted until the tank was broken or for 45,000 cycles.	Room temperature (without temperature control) High temperatures (85 °C, 95% relative humidity) Low temperature (85 °C)	4 cycles/min Cycle the pressure in the tank between less than 1 MPa and more than 125% of the normal filling pressure	The fatigue strength of the Type III tank decreases at low temperatures and increases at high temperatures; The fatigue life of the CFRP layer of a Type IV tank decreases in a high-temperature

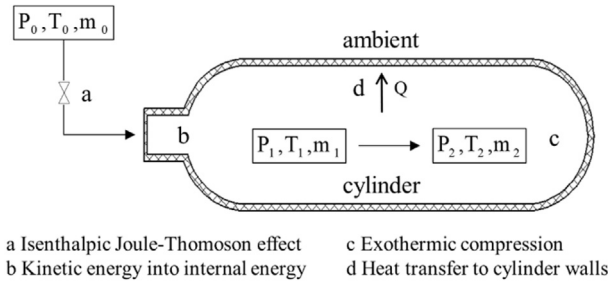


Fig. 3 – Theoretical model of filling for the composite cylinder [51].

threshold [65]. In order to ensure safety, it is necessary to study the relationship between the filling rate and the final temperature. Several typical experiments are presented in Table 8.

Short filling time reduces the time for the heat transfer between the gas and the cylinder wall to evacuate the heat accumulated in the gas. Systematic studies has been undertaken on the effect of filling time and experiments with a mount of thermocouples (type T) as shown in Fig. 4 have been conducted by Dicken et al. [62]. Based on the Spallart-Allmaras turbulence model and the real gas equation of the state, a numerical model was developed to investigate the mechanism of temperature rise and heat transfer within a type III cylinder during refueling [66]. It is found that the mass flow rate, initial pressure and inlet temperature are the main factors that affect the final temperature rise. Especially the mass flow rate has a high effect, with a high, nearly exponential, growth as the mass filling rate increases. In another research [64], the 0D gas 1D wall model shows the heat transfer is limited by the conduction in the tank wall and the temperature rise varies linearly with the filling time square root with a sensitivity coefficient of $-8.8 \text{ }^\circ\text{C}/(\text{min})^{1/2}$ at 70 MPa and $-10.6 \text{ }^\circ\text{C}/(\text{min})^{1/2}$ at 70 MPa. In addition, Zheng et al. [63] revealed that the greatest increase in temperature occurs at the start of filling due to the Joule-Thomson effect. Optimized filling strategy could be developed by using a slow filling rate

at the beginning and then higher rate later without sacrificing average fueling rate. However, this has still to be demonstrated.

Effect of inlet temperature (or feeding temperature)

In addition, cooling the gas before injecting it into the vessel is also an effective way to meet the safety requirement. Several researches were conducted as shown in Table 9. Melideo et al. [56] developed different filling strategies to study its effects on 3 key-parameters: the maximum temperature, the SOC and the theoretical cooling energy demand. For energy saving, higher SOC and lower final temperature rise, precooling the gas in the second half of the filling seems more suitable. However, Bourgeois et al. [68] showed that the most important parameter in pre-cooling is the mass average temperature of the gas at the inlet of the tank. In another work [12], based on a type IV 70 MPa vessel, Melideo et al. performed a CFD model to investigate the effects of inlet gas temperature on final temperature during the fast filling process with pre-cooling. The results show that the final gas temperature increases when the pre-cooling temperature increases. The $0 \text{ }^\circ\text{C}$ is a critical point: inlet gas temperature that higher than $0 \text{ }^\circ\text{C}$ can lead to a final temperature higher than $85 \text{ }^\circ\text{C}$.

Considering pre-cooling the gas improves the SOC value as well, a new analytical solution from a simplified lumped parameter model was proposed by Cebolla et al. [67] to determine hydrogen pre-cooling temperature from refueling parameters. Experiments were carried out at different gas flow rates and initial temperatures, coupling the two parameters to get the cross effect on the final value of SOC. The case without precooling gets a higher temperature, exceeding $85 \text{ }^\circ\text{C}$. It can be observed that the increase in the inlet temperature not only reduces the SOC, but also increases the negative impact of the flow rate on the final SOC with the result. With its 0D gas 1D wall model, it [64] shows a linear variation of the final temperature with the inlet temperature, with a sensitivity coefficient of $0.99 \text{ }^\circ\text{C}/^\circ\text{C}$ at 70 MPa and $0.88 \text{ }^\circ\text{C}/^\circ\text{C}$ at 35 MPa, but the cross effect is not characterized.

Table 6 – Theoretical analysis of temperature rise.

Team	Equations	Annotation
Liu et al. [51]	$Q = \Delta E - U_0 - W_{tot} = m_2 u_2 - m_1 u_1 - (m_2 - m_1) h_0 \frac{pv}{R_0 T} = \left(1 + \frac{\alpha p}{T}\right) T_2 =$ $\frac{\lambda \mu T_1 (T_1 + \alpha p_1) - \alpha (\lambda p_1 T_1 - p_1 T_1)}{T_1 + \alpha p_1 + \frac{\alpha T_1 p_1 - T_1 p_1}{p_2}}$	$\alpha = 1.9155 \times 10^{-6} \text{ k}/\text{Pa} \lambda = c_{p0}/c_{v2} \mu = c_{v1}/c_{v2}$
M. Hosseini et al. [52]	$m_1 u_1 + (\dot{m}_i t) h_i = m_2 u_2 + t \dot{Q} m_1 e x_1 + (\dot{m}_i t) e x_i = m_2 e x_2 + I_{filling} m_1 e x_1 +$ $(\dot{m}_i t) e x_i = m_2 e x_2 + t \dot{Q} \left(1 - \frac{T_0}{T_S}\right) + I_{1-2} \psi_{filling,1-2} = \frac{m_2 e x_2}{m_1 e x_1 + (\dot{m}_i \times t) e x_i}$	$\dot{m}_i = \frac{dm_i}{dt}$ $\dot{Q} = \frac{dQ}{dt}$
Yang et al. [53]	$dU = \delta Q - \delta W + h_e dn_e (N_i + Kt) \frac{du}{dt} + uK = \dot{Q} + h_e K$	$\psi_{filling,1-2}$: The exergy efficiency h_e : molar enthalpy of inlet hydrogen n_e : molar of gas input to the system
Wang et al. [54]	$T_2 = \frac{P_1 T_1 V + \lambda T_0 (RT_1 + \alpha TP_1) \int m dt}{P_1 V + (RT_1 + \alpha TP_1) \int m dt}$ $m_2 = \frac{P_1 P_2 V^2 + P_2 V (RT_1 + \alpha TP_1) \int m dt}{P_1 T_1 VR + \alpha P_1 P_2 VR + \lambda (RT_0 + \alpha RP_2) (RT_1 + \alpha RP_1) \int m dt}$	$\alpha = 1.9155 \times 10^{-6} \text{ k}/\text{Pa} c_v = 5.178 \text{ kJ}/(\text{kg} \cdot \text{K})$ $\lambda = c_p/c_v$

Table 7 – Researches on the effect of initial pressure on final temperature.

Team	Total volume of tanks (L) and tank's type	Ambient temperature (°C)	Initial to final pressure (MPa)	Ref.
Zheng et al.	74 (type III)	/	5.5 → 70 9.5 → 70	[7]
Liu et al.	150 (new type)	20	5 → 35 15 → 35 25 → 35	[51]
Kim et al.	72 (type IV)	20	0 → 35 5 → 35 10 → 35 15 → 35 20 → 35	[28]
Dicken et al.	40 (type III)	15	5 → 35 15 → 35 20 → 35	[62]
Zheng et al.	129 (type IV)	/	5 → 70 15 → 70 25 → 70	[63]

Table 8 – Researches on the effect of filling rate on final temperature.

Team	Year	Total volume of tanks (L) and tank' type	Initial to final pressure (MPa)	Filling rate (g/s)	Filling time (s)	Ref.
Dicken et al.	2007	74 (type 3)	10 → 35	/	40 190 370	[62]
Zhao et al.	2010	150	2 → 35	9 19 41	/	[66]
Zheng et al.	2011	129 (type 4)	70	9 19 41	/	[63]
Cebolla et al.	2015	40 (type 3)	2 → 78	2 4 6 8 10	/	[67]

Effect of cylinder dimension or cylinder type

At present, the type III and type IV are considered as most suitable solutions for on-board hydrogen storage. The inner layer of type III tank is made of aluminum, while the type IV inner layer is made of plastic (e.g. high density polyethylene).

Since the thermal conductivity of the plastic liner is smaller than that of the metal one, the heat transfer from the gas to the tank wall is slower in the type IV than in the type III and the type IV cylinder absorbs less heat. There are several researches shown in Table 10. So the temperature evolution have the same trend in both cylinders, but a lower final

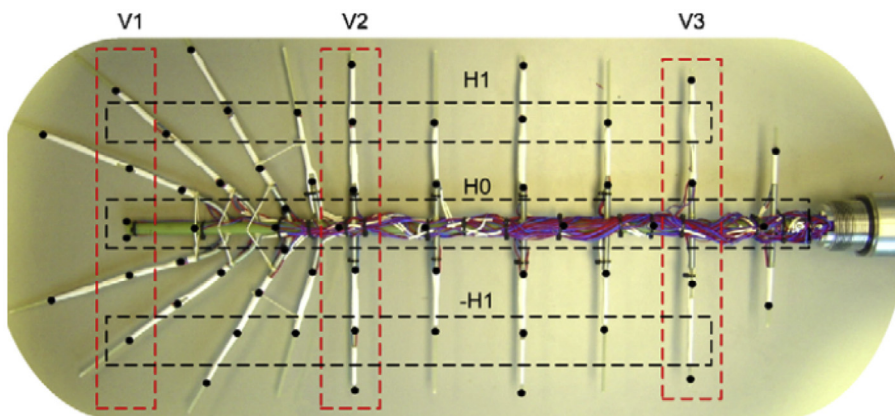


Fig. 4 – Thermocouple support mechanism [62].

Table 9 – Researches on the effect of inlet temperature on final temperature or the SOC.

Team	Year	Total volume of tanks (L) and tank' type	Initial inlet gas temperature (°C)	Filling time (s)	SOC or final temperature (% or °C)
Melideo et al.	2014	Type 4	-40	200	96%
			-20		93%
			0		91%
			15		89%
Cebolla et al.	2015	40 (type 3)	-40	/	99%
			-20		96%
			0		92%
			25		89%
Melideo et al.	2015	29 (type 4)	-40	204	58 °C
			-20		74 °C
			0		85 °C
			15		96 °C

temperature is obtained in the type III tank due to the higher thermal diffusivity of the aluminum liner with respect to the plastic liner. When the inlet temperature rise, the maximum gas temperature, reached at the end of the filling, increases linearly while the state of charge decreases linearly [69]. With similar inlet gas temperature and other boundary conditions, the final SOC is higher in a type III than in a type IV tank. Due to the effect of heat transfer, it also found that the higher the inlet gas temperature, the higher the influence of the tank type on the final SOC [67].

To study the effect of cylinder dimensions, cylinder A with 1652 mm length and 376 mm inner diameter was selected by Zheng et al. [7] to be compared with cylinder B which has a smaller length to diameter ratio. From the calculated temperature profile, shown in Fig. 5, the gas temperature in cylinder A is non-uniformly distributed and increases gradually in axial direction, the highest temperature occurs in the caudal region while the lowest is near the inlet. Cylinder B has a good temperature homogeneity that is consistent with the experimental results. According to this result, the large length to diameter ratio may cause too high local temperature, so reducing the length to diameter ratio is beneficial to cylinder safety.

Effect of initial and ambient temperature

Concerning the ambient temperature, according [61] the higher ambient temperature causes heat releasing difficulty. Therefore, the ambient temperature would also have an effect on the final temperature. But following the research [64], it is preferable to distinguish the ambient temperature (outside or external temperature) and the initial temperature of the gas

and wall tank, which, in some cases, can be different. Indeed, the initial temperature has an effect on the final temperature, whereas for the short fueling times (a few minutes) heat conduction to the outer side of the tank wall only concern a marginal part of the heat transferred to the inner part of the wall; therefore, the external temperature has a marginal effect.

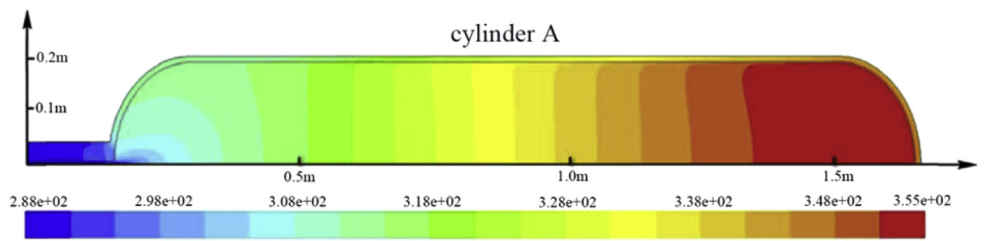
A three dimensional computation model was developed to predict the thermo-fluid dynamic behavior as shown in Table 11 [29]. The results revealed that the ambient temperature has an ignorable effect on the final temperature; but when the initial gas and wall temperature is increased, the effect become significant and the maximum temperature can exceed the safety limit. It can be concluded that the maximum temperature rise has the same trend as the initial temperature and there is a linear relationship between them. From the numerical simulations carried out by Zhao et al. [66], an increase of 1 °C in the initial temperature is followed by a growth of 0.3 °C in the maximum temperature.

CFD simulations

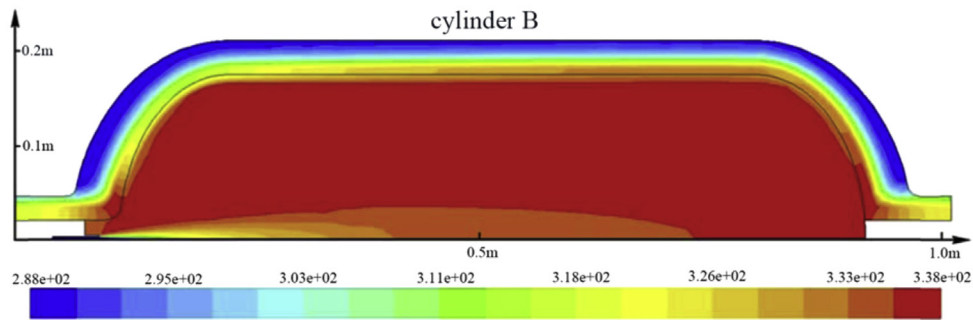
The experiments consume many workers and material resources. In addition, it may be dangerous to a certain extent. Fortunately, Computational Fluid Dynamics (CFD) codes already proved to be a valuable tool for predicting the temperature distribution within a tank during refueling [17]. The CFD simulation models should be established based on turbulence model, real gas model and heat transfer model. Moreover, the model capabilities are evaluated by sensitivity analyses of grid refinement, turbulence model, boundary

Table 10 – Researches on the effect of cylinder dimension or type on final temperature.

Team	Year	Total volume of tanks (L) and tank' type	Initial to final pressure (MPa)	Ambient temperature (°C)	Ref
Miguel et al.	2016	Type III Type IV	2 → 77	25	[69]
Cebolla et al.	2015	Type III Type IV	2 → 78/77	/	[67]
Zheng et al.	2013	150 (cylinder A) 74 (cylinder B)	2 → 35	25	[7]



(a) Temperature distribution within cylinder A



(b) Temperature distribution within cylinder B

Fig. 5 – Hydrogen temperature distribution within the cylinder at the end of refueling [7].

conditions, inlet pipe geometry, external wall heat transfer coefficient and tank material properties [17]. Many scholars have made a series of CFD simulations and validations by comparing the transient three-dimensional CFD results with experimental data for various scenarios of hydrogen filling. With using the commercially available CFD package FLUENT, CFX [70,71] the hydrogen filling process can be modeled under the given operating conditions by changing the parameters to study the effects of different temperature and pressure on the temperature rise in the cylinder. As known, the key points in CFD analysis are division of geometric grids, selection of turbulence model, gas state equation, setting of definite initial and boundary conditions and post-processing.

Geometry grid

Of course, the geometry should be the first consideration in the modeling process. From the perspective of computing resources, if the filling stage only is to be studied a two-dimensional model can be built firstly, because a three-

dimensional model needs to run completely for several weeks. Melideo et al. [56] firstly validate the possibility to use 2D axisymmetric meshes successfully for the CFD simulations of fast filling with pre-cooling. The article shows that the temperature histories for the 3D and 2D meshes are almost completely overlapping. In other words, the 2D axisymmetric approach can be used during the filling stage. However, a 3D computational mesh has to be considered after the filling is completed. Because the speed of flow is so fast that the influence of buoyancy can be neglected during the filling stage. However, the buoyancy effect becomes more relevant in the holding time and during the emptying process due to the low flow velocity. Thus, the 3D might be more appropriate if we look at the whole process. Also considering only half of the geometry for the CFD simulations is an effective strategy to reduce the computer run-time. Melideo et al. [72] performed simulations with the whole 3D geometry and with half of the geometry and gave the fact that the effects of that approach on the temperature histories are negligible.

Table 11 – Researches on the effect of initial temperature.

Team	Year	Total volume of tanks (L) and tank' type	Initial to final pressure (MPa)	Initial temperature (°C)	Ref
Suryan et al.	2012	74 (type 3)	9.3 → 35	20.4 40.4 50.4	[29]
Zhao et al.	2010	150	2 → 35	-10 0 10 20 30 40	[66]

Table 12 – Turbulence model.

Name	Model
Realizable k-ε model	$\frac{\partial(\rho k)}{\partial t} + \frac{\partial(\rho k u)}{\partial x_i} = \frac{\partial}{\partial x_i} \left[\left(\mu + \frac{\mu_t}{\sigma_k} \right) \frac{\partial k}{\partial x_j} \right] + Gk + Gb - \rho \epsilon - YM,$ $\frac{\partial(\rho \epsilon)}{\partial t} + \frac{\partial(\rho \epsilon u)}{\partial x_j} = \frac{\partial}{\partial x_j} \left[\left(\mu + \frac{\mu_t}{\sigma_\epsilon} \right) \frac{\partial \epsilon}{\partial x_j} \right] + \rho 1C1Se - \rho C2 \frac{\epsilon^2}{k + \sqrt{b\epsilon}}$
Renormalization group k-ε model	$\frac{\partial(\rho k)}{\partial t} + \frac{\partial(\rho k u_i)}{\partial x_i} = \frac{\partial}{\partial x_j} \left(\alpha k \mu_{eff} \frac{\partial k}{\partial x_j} \right) + Gk + Gb + Sk - \rho \epsilon - YM,$ $\frac{\partial(\rho \epsilon)}{\partial t} + \frac{\partial(\rho \epsilon u_i)}{\partial x_i} = \frac{\partial}{\partial x_j} \left(\alpha k \mu_{eff} \frac{\partial \epsilon}{\partial x_j} \right) + C1 \frac{\epsilon}{k} (GK + C3rGb) + Sr - \rho C2r \frac{\epsilon^2}{k}$
Shear stress transport k-ω model	$\frac{\partial(\rho \epsilon)}{\partial t} + \frac{\partial(\rho \epsilon u)}{\partial x_i} = \frac{\partial}{\partial x_j} \left(\alpha k \mu_{eff} \frac{\partial \epsilon}{\partial x_j} \right) + C1 \frac{\epsilon}{k} (GK + C3rGb) + Sr - \rho C2r \frac{\epsilon^2}{k}$ $\frac{\partial(\rho k)}{\partial t} + \frac{\partial(\rho k u)}{\partial x_i} = \frac{\partial}{\partial x_j} \left(r k \frac{\partial k}{\partial x_j} \right) + Gk - \beta \rho k \omega$ $\frac{\partial(\rho \omega)}{\partial t} + \frac{\partial(\rho \omega u_i)}{\partial x_i} = \frac{\partial}{\partial x_j} \left(r k \frac{\partial k}{\partial x_j} \right) + G\omega - \beta \rho \omega^2 + D\omega$ $\frac{\partial}{\partial t} (\rho \overline{u' u' j}) + \frac{\partial}{\partial x_k} (\rho u_k \overline{u' u' j}) = - \frac{\partial}{\partial x_k} [\rho \overline{u' u' j u' k} + \rho (\delta_{kj} \overline{u' i} + \delta_{ki} \overline{u' j})] + \frac{\partial}{\partial x_k} \left[\mu \frac{\partial}{\partial x k} (\overline{u' u' j}) \right]$ $- \rho \left(\overline{u' u' k} \frac{\partial u_j}{\partial x k} + \overline{u' j u' k} \frac{\partial u_i}{\partial x k} \right) - \rho \beta \left(\overline{g i u' j} \rho + g j u' j \rho \right)$
Reynolds stress model	

Table 13 – Real gas equations.

Name	Equations
Redlich-Kwong equation	$p = \frac{RT}{\sqrt{m-b}} - \frac{a}{\sqrt{TVm}(Vm+b)}$
Soave's modified Redlich-Kwong equation	$p = \frac{RT}{\sqrt{m-b}} - \frac{a\alpha}{Vm(Vm+b)}$
Aungier's modified Redlich-Kwong equation	$p = \frac{RT}{\sqrt{m-b+c}} - \frac{a}{Vm(Vm+b)T_r^q}$
Peng-Robinson equation	$p = \frac{RT}{\sqrt{m-b}} - \frac{a\alpha}{V^2m + 2bVm - b^2}$

Grid quality directly affects the rationality and correctness of CFD simulation results. Generally, the finer the mesh, the more accurate the result is, but the longer time the calculations take. It is reasonable to draw as few grid cells as possible on the premise of accuracy. And Kim et al. [28] made a simple comparison between the results with 300,000 cells of hybrid mesh and with 600,000 cells of tetrahedral mesh. Finally, the results show the effect of the grid resolution on the accuracy was minimal in this study.

Turbulence models

CFD is a numerical solution to the Navier–Stokes (N–S) equations to obtain all the variables of the full field. The addition of Reynolds stress equation in the N–S equations of turbulence makes the equation system unclosed. Therefore, a corresponding turbulence model has been established to be able to solve the whole flow field. The governing model suitable for hydrogen flows needs to be determined. Four different kinds of turbulence models are summarized as shown in Table 12. Suryan et al. [73] compared the consistency between simulation results of different turbulence models in CFD and experiments. The realizable $k-\epsilon$ model and the Reynolds Stress Model were identified as the most suitable turbulence models for the simulation of hydrogen gas fast filling process.

The unsteady Favre averaged Navier–Stokes equations are given by Ref. [74].

$$\frac{\partial \rho}{\partial t} + \nabla \cdot (\rho \vec{v}) = 0 \quad (1)$$

$$\frac{\partial}{\partial t} (\rho \vec{v}) + \nabla \cdot (\rho \vec{v} \vec{v}) = -\nabla p + \nabla \cdot (\bar{\tau}) + \rho g \quad (2)$$

$$\frac{\partial}{\partial t} (\rho E) + \nabla \cdot (\vec{v} (\rho E + p)) = \nabla \cdot (k_{eff} \nabla T + (\bar{\tau}_{eff} \cdot \vec{v})) \quad (3)$$

Real gas model

The system of N–S equations and turbulence model equations has to be closed with an equation of state for the hydrogen gas. The ideal gas model is suitable for most engineering flows. However, the compressibility effects are significant in the hydrogen tank filling and at high pressure the hydrogen gas may deviate from ideal gas behavior. Therefore, a suitable real gas model has to be chosen. In Suryan's other articles [29], four real gas equations are offered as shown Table 13 [75–78] and their validity is verified.

Definite conditions

The definite conditions (initial conditions and boundary conditions) are the premises that the governing equations have a definite solution. Thus, based on the research on CFD model analysis, the information shown in Table 14 is summarized.

The safety and fast filling strategies

How to refuel safely and fast becomes a significant issue with the large-scale development of FCVs. The SAE J2601 protocol was developed to ensure that 5–7 kg of hydrogen could be safely filled into FCVs within 3–5 min from the station. The safety limits of the vehicle storage system are shown in Table 15 [80]. The fueling protocol determines the fueling average pressure ramp rate (APRR) at the dispenser, which is affected by the hydrogen precooling temperature at the dispenser, the vehicle tank volume and tank initial pressure, and the ambient temperature. There are two fueling methods involved in this protocol, known as the “lookup table” method and the “MC formula” method. The lookup table method provides a fixed end-of-fill pressure target. The MC method is the dynamic control of the APRR, taking advantage of the thermodynamic properties of the hydrogen tank to calculate the pressure target continuously. The current standard method of fueling for FCVs is the lookup table method. However, the “MC formula” method has a greater advantage in reducing fueling time in certain conditions. Reddi et al. employ a physical model to compare the fueling performance of two fueling methods [81].

In order to reduce the final temperature and minimize the energy consumption for hydrogen compression, three effective control strategies of fast filling are proposed via the analysis of the relationships between temperature rise and filling parameters above. The first method is controlling the mass flow rate accurately in the filling process: slow at first and then faster. The second method is that the cylinder can be refueled with a multi-level storage system, which is composed of several hydrogen storage vessels with staged initial pressures. The last method is adjusting the hydrogen pre-cooling temperature by analyzing the refueling parameters.

Filling rate control strategy

In order to achieve a short refueling time, the filling rate must be controlled in an appropriate range. However, the temperature rise has a high growth as the mass filling rate increases compared to other parameters. Therefore, accurate filling rate control is particularly important to satisfy both filling time and the temperature rise.

The filling rate has a remarkable effect on the temperature rise. Therefore, varying the filling rate could control the temperature better than the constant flow rate. It can be seen from a large number of experiments and simulation results that the gas temperature in the cylinder increases sharply at first and then slowly when all the filling parameters are kept constant like Fig. 6 [11]. Temperature rise mainly occurs in the first quarter of the filling time [82]. Therefore, the mass flow rate may be controlled slowly at first and then fast without

Table 14 – Summary of CFD simulations.

Author	Tank	Boundary and initial conditions	Geometry and computational grid	Turbulence model	Real gas equation
Sung Chan Kim [28]	72 L 35 MPa	Boundary: Inlet: the mass flow rate Initial conditions: Temperature: 17 °C	Gas: hexahedral solid volume: tetrahedral	Standard k- ϵ turbulence	Redlich-Kwong
M. Heitsch [57]	74 L 35 MPa	Boundary: mass flow rate, experimental pressure and temperature Initial conditions: quiescent flow conditions	Gas domain: tetrahedra and pyramids Liner and insulation: hexahedral	SST	Redlich-Kwong
M. Cristina Galassi [17]	29 L 70 MPa	Boundary: solid interface: non-slip Tank inlet: experimental pressure and temperature Initial conditions: experimental temperature and pressure	Inlet pipe and solid domains: hexahedral fluid domain: tetrahedral	A modified k- ϵ model	Redlich-Kwong
Abhilash Suryan [29]	74 L 35 MPa	Boundary: experimental pressure and temperature Initial conditions: pressure 9.3 MPa and temperature 293.4 K	Fluid domain: 209,190 hexahedral. Solid domain: 96,510 hexahedral	(SST) k- ω turbulence model	Four real gas equations
Abhilash Suryan [73]	74 L 35 MPa	Boundary: experimental inlet conditions tank inside wall: no-slip condition Initial conditions: pressure 9.3 MPa and temperature 293.4 K	Fluid domain: 16752 quadrilateral Solid domain: 6304 quadrilateral	Comparison of four turbulence models	Redlich-Kwong
Daniele Melideo [56]	28.9 L 2–77.5 MPa	Boundary: All walls: non-slip boundary condition. Tank inlet: experimental pressure and temperature Initial conditions: initial temperature and pressure (p = 2.2 MPa, T = 15 °C)	3D Inlet pipe and solid domains: hexahedral fluid domain: tetrahedral 2D axial symmetry;	A modified k- ϵ model	Aungier's modified Redlich-Kwong equation
D. Melideo [72]	40 L 75 MPa	Initial conditions: experiment initial tank temperature and pressure	3D Only half of the geometry	A modified k- ϵ approach	Redlich-Kwong
M. Cristina Galassi [79]	70 MPa	Boundary: Inner tank and inlet pipe: non-slip boundary condition. Initial conditions: H2 initial temperature (291 K) and gage pressure (0.2 bar)	Four different 3D computational with various mesh refinements	A modified k- ϵ model	Redlich-Kwong

Table 15 – SAE-J2601 performance and safety limits for hydrogen vehicle tank fueling.

Parameter	Limits
Hydrogen storage system capacity	35 MPa: 1.2–6 kg 70 MPa: 2–10 kg
Ambient temperature scope	–40 °C–50 °C
Gas temperature scope	–40 °C–85 °C
Dispenser pressure scope	0.5 MPa–8.5 MPa
Maximum flow rate	60 g/s
Maximum hydrogen mass during Startup	200 g

increasing the overall filling time. However, the optimized mass flow rate variation requires further research according to different initial parameters.

Refueling with multi-stage initial pressures

According to the investigations carried out by the researchers, another fast filling strategy is summarized: filling with multi-stage initial pressure. Firstly, it greatly reduces the energy consumption to compress the hydrogen with three different pressure tanks respectively; moreover, it also fits with the above strategy, which requires a slow filling rate at first and then a faster filling rate. The diagram of filling process is shown as Fig. 7.

The multi-stage refueling strategy has been investigated by several researchers so far and gradually gets a wide application in hydrogen stations. With the same cylinder, the difference is that there are multi-stage pressure storage tanks in the filling process. As known, the consumption of compressing the hydrogen declines with the increase of pressure stages. Nevertheless, the cost of the equipment is higher and the control strategy is more complex, which may reduce the reliability of the system. Therefore, a three-stage pressure storage process appears relatively reasonable. In this refueling process, the cylinder is filled by the three tanks in the order of low-pressure tank, medium-pressure tank and high-pressure tank [13].

To investigate the optimal pressures of the three storages and the fast filling strategy, Zheng et al. [83] quantified the

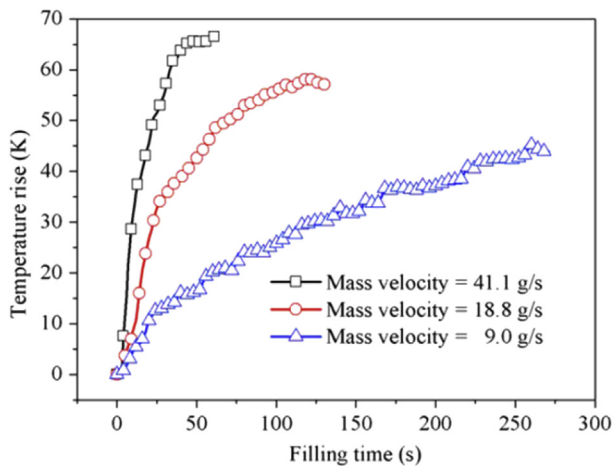


Fig. 6 – Temperature rise in the case of different mass filling rate [11].

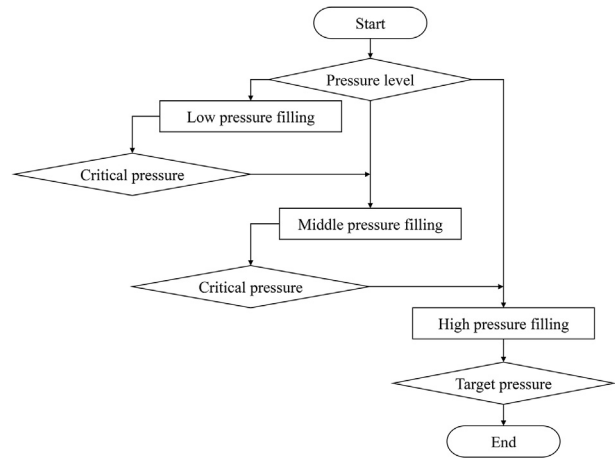


Fig. 7 – The diagram of multi-stage filling [13].

hydrogen utilization ratio and the filling time and proposed a two-objective optimization model. Based on the two-objective optimization model, an optimized filling algorithm is proposed to achieve a high hydrogen utilization ratio and a fast filling; the optimization algorithm was validated by two examples. Soon afterwards, the temperature rise within a 70 MPa type III cylinder with this strategy was studied in another paper. The equipment used in this experiment is shown in Fig. 8 and the results show that the experiment system with pre-cooling can meet the requirements of the 70 MPa hydrogen fast refueling.

Determining pre-cooling temperature from refueling parameters

At present, hydrogen pre-cooling is the most effective solution to reduce the temperature rise for fast filling. Nevertheless, as the initial pressure and initial temperature of each hydrogen cylinder are various with each of the different vehicles, whether the hydrogen needs to be pre-cooled or the pre-cooling temperature are unknown; furthermore, energy savings can be achieved if the initial conditions of the tank are correctly identified. Therefore, developing a strategy to predict the pre-cooled temperature according to the initial parameters is imperative.

In order to obtain the relationship between the precooling temperature and the filling parameters, a model of fast filling should be developed, including the filling parameters. Then, according to the large amount of data collected, the fitting formula that helps to determine the pre-cooling temperature could be obtained. A numerical solution for the lumped parameter thermodynamic model of adsorptive and cryo-adsorptive hydrogen storage systems was developed by Xiao et al. [84]. Based on the parameter thermodynamic model associated with the reference data during the filling process, the simple fitting formula is developed. They investigated the pre-cooling temperature determined from initial pressure and final pressure, filling time and final pressure and initial temperature and final pressure respectively. It is validated that the fittings agreed well with the experiment data. In brief, the pre-cooling hydrogen temperature could be well determined

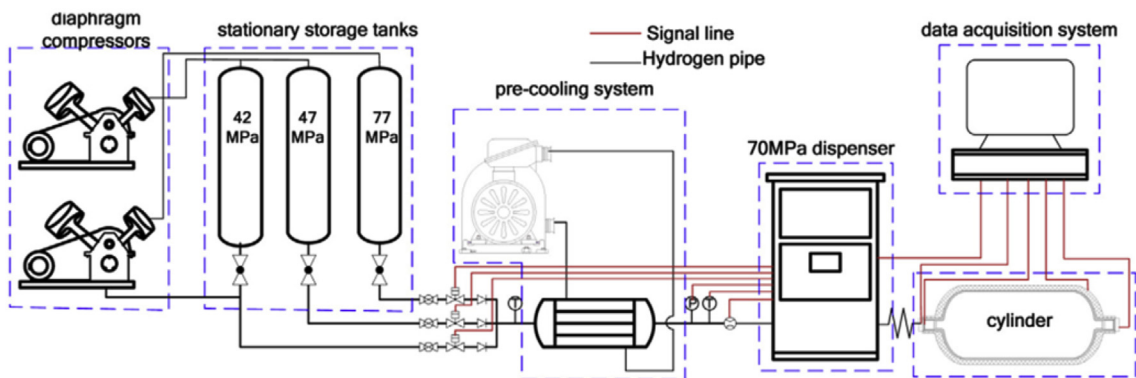


Fig. 8 – Schematic diagram of experimental apparatus [7].

and the safety during the filling process may be ensured with this method.

Conclusion

In summary, multiple techniques of hydrogen storage are feasible for transportation storage and bulk stationary storage. However, the different hydrogen storage methods have their best application fields and the compressed hydrogen is more popular and suitable in the transportation domain due to its ease of carrying, ease of use, acceptable efficiency and mature technology. Currently, type III and IV cylinders are mainly used in vehicles due to their merit of lightweight and high mechanical strength. However, the violent changes of temperature will cause thermal stress, which may lead to significant laminate damages in the form of micro cracks in the resin and further result to composite failure, when added to the stresses caused by internal pressure.

It is observed that the temperature rises and SOC are affected by several parameters. However, controlling the parameters such as initial temperature, type of hydrogen storage cylinder and initial pressure in the tank is not significant for the different areas or vehicles, so the optimal control of initial inlet gas temperature and filling rate are particularly important. Precooling the hydrogen is an ideal method to decrease the initial inlet gas temperature. The targets of final temperature and filling time are achieved by coupling the control of cooling temperature and filling rate. In view of the reality, some numerical simulations based on experimental data were performed to verify the CFD. The boundary conditions, initial conditions and CFD simulation model, based on turbulence model, real gas model and heat transfer model are set to verify the validity of the model. Considering the effective parameters on the temperature rise and SOC, three fast filling strategies are reviewed: filling rate control strategy, refueling with multi-stage initial pressures and determining pre-cooling temperature from refueling parameters proposed. All of them are validated effective and the further study is coupling the three strategies to obtain an optimal multi-stage filling strategy which may decrease the temperature rise and reduce the energy consumption.

Acknowledgments

This work is supported in part by the National Key Research And Development Program (No.: 2018YFB0105703 and No.: 2018YFB0105402), the National Nature Science Foundation of China (51806024), the Chongqing Research Program of Foundation and Advanced Technology (No.: cstc2017jcyjAX0276) and Research Projects of Chongqing University, China (No.:106112017CDJPT280005, No.: 106112016CDJXZ338825 and No.: 106112017CDJQJ338812).

REFERENCES

- [1] Daud WRW, Rosli RE, Majlan EH, Hamid SAA, Mohamed R. PEM fuel cell system control: a review. *Renew Energy* 2017;113.
- [2] Rakhtala SM, Roudbari ES. Application of PEM fuel cell for stand-alone based on a Fuzzy PID control. *Bulletin EEI* 2016;5.
- [3] Erdinc O, Uzunoglu M. Recent trends in PEM fuel cell-powered hybrid systems: investigation of application areas, design architectures and energy management approaches. *Renew Sustain Energy Rev* 2010;14:2874–84.
- [4] Gencoglu MT, Ural Z. Design of a PEM fuel cell system for residential application. *Int J Hydrogen Energy* 2009;5242–8.
- [5] Gurz M, Baltacioglu E, Hames Y, Kaya K. The meeting of hydrogen and automotive: a review. *Int J Hydrogen Energy* 2017;42:23334–46.
- [6] Acosta B, Moretto P, Miguel ND, Ortiz R, Harskamp F, Bonato C. JRC reference data from experiments of on-board hydrogen tanks fast filling. *Int J Hydrogen Energy* 2014;39:20531–7.
- [7] Zheng J, Guo J, Yang J, Zhao Y, Zhao L, Pan X, et al. Experimental and numerical study on temperature rise within a 70MPa type III cylinder during fast refueling. *Int J Hydrogen Energy* 2013;38:10956–62.
- [8] Krishna R, Titus E, Salimian M, Okhay O, Rajendran S, Rajkumar A. Hydrogen storage for energy Application. 2012.
- [9] Johnson T, Bozinoski R, Ye J, Sartor G, Zheng J, Yang J. Thermal model development and validation for rapid filling of high pressure hydrogen tanks. *Int J Hydrogen Energy* 2015;40:9803–14.
- [10] Mori D, Hirose K. Recent challenges of hydrogen storage technologies for fuel cell vehicles. *Int J Hydrogen Energy* 2009;34:4569–45742.

- [11] Liu YL, Zhao YZ, Zhao L, Li X, Chen HG, Zhang LF, et al. Experimental studies on temperature rise within a hydrogen cylinder during refueling. *Int J Hydrogen Energy* 2010;35:2627–2632.
- [12] Melideo D, Baraldi D. CFD analysis of fast filling strategies for hydrogen tanks and their effects on key-parameters. *Int J Hydrogen Energy* 2015;40:735–45.
- [13] Guo J, Xing L, Hua Z, Gu C, Zheng J. Optimization of compressed hydrogen gas cycling test system based on multi-stage storage and self-pressurized method. *Int J Hydrogen Energy* 2016;41:16306–15.
- [14] Reddi K, Elgowainy A, Sutherland EJ. Hydrogen refueling station compression and storage optimization with tube-trailer deliveries. *Int J Hydrogen Energy* 2014;39:19169–81.
- [15] Xiao W, Cheng Y, Lee WJ, Chen V, Charoensri S. Hydrogen filling station design for fuel cell vehicles. *IEEE T Ind Appl* 2011;vol. 47:245–51.
- [16] Parks G. Hydrogen station compression, storage, and dispensing technical status and costs. National Renewable Energy Laboratory; 2014.
- [17] Galassi MC, Baraldi D, Iborra BA, Moretto P. CFD analysis of fast filling scenarios for 70MPa hydrogen type IV tanks. *Int J Hydrogen Energy* 2012;37:6886–92.
- [18] Dutta S. A review on production, storage of hydrogen and its utilization as an energy resource. *Journal of Industrial & Engineering Chemistry* 2014;20:1148–56.
- [19] Barthelemy H, Weber M, Barbier F. Hydrogen storage: recent improvements and industrial perspectives. *Int J Hydrogen Energy* 2016;42.
- [20] Coquel F, Marmignon C. Review of hydrogen storage techniques for onboard vehicle applications. *Int J Hydrogen Energy* 2013;38:14595–617.
- [21] Abdalla AM, Hossain S, Nisfandy OB, Azad AT, Dawood M, Azad AK. Hydrogen production, storage, transportation and key challenges with applications: a review. *Energy Convers Manag* 2018;165:602–27.
- [22] James B. Overview of hydrogen storage technologies. 2008.
- [23] Züttel A. Hydrogen storage methods. *Naturwissenschaften* 2004;91:157–72.
- [24] Ren J, Musyoka NM, Langmi HW, Mathe M, Liao S. Current research trends and perspectives on materials-based hydrogen storage solutions: a critical review. *Int J Hydrogen Energy* 2017;42:289–311.
- [25] Sakintuna B, Lamari-Darkrim F, Hirscher M. Metal hydride materials for solid hydrogen storage: a review. *Int J Hydrogen Energy* 2007;32:1121–40.
- [26] Züttel A. Materials for hydrogen storage. *Mater Today* 2003;6:24–33.
- [27] Xiao J, Bénard P, Chahine R. Estimation of final hydrogen temperature from refueling parameters. *Int J Hydrogen Energy* 16 March 2017;42(11):7521–8.
- [28] Kim SC, Lee SH, Yoon KB. Thermal characteristics during hydrogen fueling process of type IV cylinder. *Int J Hydrogen Energy* 2010;35:6830–5.
- [29] Suryan A, Kim HD, Setoguchi T. Three dimensional numerical computations on the fast filling of a hydrogen tank under different conditions. *Int J Hydrogen Energy* 2012;37:7600–11.
- [30] Zheng J, Li L, Chen R, Xu P, Kai F. High pressure steel storage vessels used in hydrogen refueling station. *J Press Vessel Technol* 2008;130:244–54.
- [31] Miguel ND, Cebolla RO, Acosta B, Moretto P, Harskamp F, Bonato C. Compressed hydrogen tanks for on-board application: thermal behaviour during cycling. *Int J Hydrogen Energy* 2015;40:6449–58.
- [32] Simonovski I, Baraldi D, Melideo D, Acosta-Iborra B. Thermal simulations of a hydrogen storage tank during fast filling. *Int J Hydrogen Energy* 2015;40:12560–71.
- [33] Guo J, Yang J, Zhao Y, Pan X, Zhang L, Zhao L, et al. Investigations on temperature variation within a type III cylinder during the hydrogen gas cycling test. *Int J Hydrogen Energy* 2014;39:13926–34.
- [34] Moriya T. Develop of the FCX fuel cell vehicle at Honda 2003;27:91–6.
- [35] Bono T, Kizaki M, Mizuno H, Nonobe Y, Takahashi T, Matsumoto T, et al. Development of new TOYOTA FCHV-adv fuel cell system. *Sae International Journal of Engines* 2009;2:948–54.
- [36] Yamashita A, Kondo M, Goto S, Ogami N. Development of high-pressure hydrogen storage system for the Toyota “Mirai”. SAE 2015 World Congress & Exhibition; 2015.
- [37] Wikipedia. Hyundai Nexo. 2018. https://en.wikipedia.org/wiki/Hyundai_Nexo.
- [38] Wikipedia. Hyundai ix35 FCEV. 2018. https://en.wikipedia.org/wiki/Hyundai_ix35_FCEV.
- [39] Hyundai. All-new Hyundai NEXO – the future utility vehicle made by Hyundai. 2018. <https://www.hyundai.news/eu/press-kits/all-new-hyundai-nexo-the-future-utility-vehicle-made-by-hyundai/>.
- [40] Driver Ca. Toyota Mirai. 2018. <https://www.caranddriver.com/toyota/mirai>.
- [41] Hyundai. ix35 Fuel cell realizing the dream of a clean environment. 2018. <http://www.hyundai.com/eu/en/Showroom/Eco/ix35-Fuel-Cell/PIP/index.html>.
- [42] Wikipedia. Honda clarity. 2018. https://en.wikipedia.org/wiki/Honda_Clarify.
- [43] Toyota. Toyota Mirai technical specifications vs FCHV-adv. 2018. https://en.wikipedia.org/wiki/Honda_Clarify.
- [44] Hyundai. ix35 Fuel cell. 2018. <https://www.hyundai.com/worldwide/en/eco/ix35-fuelcell/highlights>.
- [45] Darling RM, Meyers JP. Kinetic model of platinum dissolution in PEMFCs. *J Electrochem Soc* 2003;150:A1523–7.
- [46] Tomioka J-i, Kiguchi K, Tamura Y, Mitsuishi H. Influence of temperature on the fatigue strength of compressed-hydrogen tanks for vehicles. *Int J Hydrogen Energy* 2011;36:2513–9.
- [47] Camara S, Bunsell AR, Thionnet A, Allen DH. Determination of lifetime probabilities of carbon fibre composite plates and pressure vessels for hydrogen storage. *Int J Hydrogen Energy* 2011;36:6031–8.
- [48] Zheng C-x, Wang L, Li R, Wei Z-x, Zhou W-w. Fatigue test of carbon epoxy composite high pressure hydrogen storage vessel under hydrogen environment. *J Zhejiang Univ - Sci* 2014;14:393–400.
- [49] Comond O, Perreux D, Thiebaud F, Weber M. Methodology to improve the lifetime of type III HP tank with a steel liner. *Int J Hydrogen Energy* 2009;34:3077–90.
- [50] Tomioka JI, Kiguchi K, Tamura Y, HJ Mitsuishi. Influence of pressure and temperature on the fatigue strength of Type-3 compressed-hydrogen tanks. *Int J Hydrogen Energy* 2012;37:17639–44.
- [51] LIU YanLei, ZHAO YongZhi, Zhao L, Xiang LI, et al. Experimental studies on temperature rise within a hydrogen cylinder during refueling. *Int J Hydrogen Energy* 2010;35:2627–32.
- [52] Hosseini M, Dincer I, Naterer GF, Rosen MAJJoHE. Thermodynamic analysis of filling compressed gaseous hydrogen storage tanks. *Int J Hydrogen Energy* 2012;37:5063–71.
- [53] Yang JC. A thermodynamic analysis of refueling of a hydrogen tank. *Int J Hydrogen Energy* 2009;34:6712–67214.
- [54] Wang G, Zhou J, Hu S, Dong S, Wei P. Investigations of filling mass with the dependence of heat transfer during fast filling of hydrogen cylinders. *Int J Hydrogen Energy* 2014;39:4380–8.
- [55] Monde M, Kosaka M. Understanding of thermal characteristics of fueling hydrogen high pressure tanks and

- governing parameters. *SAE Int J Alternative Powertrains* 2013;2:61–7.
- [56] Melideo D, Baraldi D, Galassi MC, Cebolla RO, Iborra BA, Moretto P. CFD model performance benchmark of fast filling simulations of hydrogen tanks with pre-cooling. *Int J Hydrogen Energy* 2014;39:4389–95.
- [57] Heitsch M, Baraldi D, Moretto P. Numerical investigations on the fast filling of hydrogen tanks. *Int J Hydrogen Energy* 2011;36:2606–12.
- [58] GTR. Proposal for a global technical regulation on hydrogen and fuel cell vehicles. 2013.
- [59] J2579 ST. Technical information report for fuel systems in fuel cell and other hydrogen vehicles. 2008.
- [60] Gaseous hydrogen and hydrogen blends land vehicle fuel tanks.
- [61] Cheng J, Xiao J, Bénard P, Chahine R. Estimation of final hydrogen temperatures during refueling 35 MPa and 70 MPa tanks ☆. *Energy Procedia* 2017;105:1363–9.
- [62] Dicken CJB, Mérida W. Measured effects of filling time and initial mass on the temperature distribution within a hydrogen cylinder during refuelling. *J Power Sources* 2007;165:324–36.
- [63] Zheng J, Liu X, Xu P, Liu P, Zhao Y, Yang J. Development of high pressure gaseous hydrogen storage technologies. *Int J Hydrogen Energy* 2011;37:1048–57.
- [64] Grouset DRC. Temperature evolutions during high pressure hydrogen tank refuelling: modelling and time scale analysis. Singapore: Hypothesis XIII symposium; 2017.
- [65] Li Q, Zhou J, Chang Q, Wei X. Effects of geometry and inconstant mass flow rate on temperatures within a pressurized hydrogen cylinder during refueling. *Int J Hydrogen Energy* 2012;37:6043–52.
- [66] Zhao L, Liu Y, Yang J, Zhao Y, Zheng J, Bie H, et al. Numerical simulation of temperature rise within hydrogen vehicle cylinder during refueling. *Int J Hydrogen Energy* 2010;35:8092–100.
- [67] Cebolla RO, Acosta B, Miguel ND, Moretto P. Effect of precooled inlet gas temperature and mass flow rate on final state of charge during hydrogen vehicle refueling. *Int J Hydrogen Energy* 2015;40:4698–706.
- [68] Bourgeois T, Brachmann T, Barth F, Ammouri F, Baraldi D, Melideo D, et al. Optimization of hydrogen vehicle refuelling requirements. *Int J Hydrogen Energy* 2017;42:13789–809.
- [69] Miguel ND, Acosta B, Baraldi D, Melideo R, Cebolla RO, Moretto P. The role of initial tank temperature on refuelling of on-board hydrogen tanks. *Int J Hydrogen Energy* 2016;41:8606–15.
- [70] CFX 11. ANSYS Inc. Southpointe, 275 Technology Drive Canonsburg. USA.
- [71] FLUENT 6.2. Fluent Inc; 2003.
- [72] Melideo D, Baraldi D, Acosta-Iborra B, Cebolla RO, Moretto P. CFD simulations of filling and emptying of hydrogen tanks. *Int J Hydrogen Energy* 2016;42:7304–13.
- [73] Suryan A, Kim HD, Setoguchi T. Comparative study of turbulence models performance for refueling of compressed hydrogen tanks. *Int J Hydrogen Energy* 2013;38:9562–9.
- [74] Menter F. Zonal two equation k-w turbulence models for aerodynamic flows, 93. Nasa STI/RECON Technical Report N; 1993.
- [75] Aungier RH. Fast, accurate real gas equation of state for fluid dynamic analysis applications. *J Fluids Eng* 1995;117:277–81.
- [76] Peng DY, Robinson DB. A New Two-Constant Equation of State, 12. *Minerva Ginecologica*; 1976. p. 3069–78.
- [77] Pitzer KS, Lippmann DZ, Curl RF, Huggins CM, Petersen DE. The volumetric and thermodynamic properties of fluids. II. Compressibility factor, vapor pressure and entropy of vaporization 1. *J Am Chem Soc* 1955;77:3433–40.
- [78] Redlich O, Kwong JN. On the thermodynamics of solutions; an equation of state; fugacities of gaseous solutions. *Chem Rev* 1949;44:233.
- [79] Galassi MC, Papanikolaou E, Heitsch M, Baraldi D, Iborra BA, Moretto P. Assessment of CFD models for hydrogen fast filling simulations. *Int J Hydrogen Energy* 2014;39:6252–60.
- [80] Engineers SoA. Fueling protocols for light duty gaseous hydrogen surface vehicles (standard J2601_201407). SAE International; 2014.
- [81] Reddi K, Elgowainy A, Rustagi N, Gupta E. Impact of hydrogen SAE J2601 fueling methods on fueling time of light-duty fuel cell electric vehicles. *Int J Hydrogen Energy* 2017;42:16675–85.
- [82] Dicken CJB, Mā©Rida WJAMR. Temperature distribution within a compressed gas cylinder during fast filling. *Adv Mater Res* 2007;15–17:281–6.
- [83] Zheng J, Ye J, Yang J, Tang P, Zhao L, Kern M. An optimized control method for a high utilization ratio and fast filling speed in hydrogen refueling stations. *Int J Hydrogen Energy* 2010;35:3011–7.
- [84] Xiao J, Wang X, Bénard P, Chahine R. Determining hydrogen pre-cooling temperature from refueling parameters. *Int J Hydrogen Energy* 2016;41:16316–21.